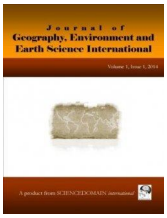

*Journal of Geography, Environment and Earth Science International*

*14(2): 1-14, 2018; Article no.JGEESI.38748*
*ISSN: 2454-7352*

# Heat Flow of Basement Adjacent to the Sergipe-Alagoas Sedimentary Basin (Northeast Brazil) from the Aeromagnetic Data and Curie Depth

**Alanna Costa Dutra[1*], Roberto Max de Argollo[1] and Alexandre Barreto Costa[1]**

*[1]Department of Earth Physics and Environment, Physics Institute, Federal University of Bahia, Brazil.*

***Authors' contributions***

*This work was carried out in collaboration between all authors. Author ACD designed the study, performed the statistical and magnetic analysis of data and wrote the first draft of the manuscript. Authors RMA and ABC performed the geothermal analysis of the study. Authors ACD and ABC managed the literature searches. All authors read and approved the final manuscript.*

***Article Information***

DOI: 10.9734/JGEESI/2018/38748
Editor(s):
(1) Pere Serra Ruiz, Department of Geography, Universitat Autònoma de Barcelona, Spain.
(2) Masum A. Patwary, Geography and Environmental Science, Begum Rokeya University, Bangladesh.
Reviewers:
(1) José Martínez Reyes, University of the Ciénega of Michoacán State, México.
(2) Kadiri Umar Afegbua, Centre for Geodesy and Geodynamics, Nigeria.
Complete Peer review History: http://www.sciencedomain.org/review-history/23823

***Original Research Article***

***Received 11th December 2017***
***Accepted 28th February 2018***
***Published 26th March 2018***

## ABSTRACT

The present project aims at the processing and interpretation of magnetic data along the basement adjacent to the Sergipe-Alagoas Sedimentary, Southern Borborema Province, and northeast Brazil. The magnetic and geological studies were developed simultaneously to make a magnetic modeling of the crustal domains and their tectonic relationships to construct a model of the geothermal structure of the crust for the region. The first part of the study consisted in to delineate contacts and border of the geologic formation. These magnetic sources have signals with various amplitudes that originate from different geometric sources, situated at different depths and with different magnetic properties. The second part consisted in to estimate of the depth of the main domains and Curie point in the study region and the knowledge of the Curie depth allows the subsequent estimation of the geothermal gradient and thermal flow in the region. The results obtained from the analysis of the magnetic anomalies shows the Curie point depth of from the 13 up to 33 km. The Curie point depth indicates the bottom depth of magnetic sources and reflects the thermal gradient and the

**Corresponding author: E-mail: alannacd@ufba.br;*

observed heat flow data. The thermal gradient varies from the 15°C/km up to 35°C/k and the heat flow varies from the 38 mW/m² up to 90 mW/m² heat flow. We compared results to the available the layers carry a magnetic signature and plunge at a significant angle, a detailed magnetic investigation was used to map the very precise surface geology. The present result was compared with the tectonic and heat flow data.

*Keywords: Sedimentary basin; curie depth; heat flow; thermal gradient; aeromagnetic data.*

## 1. INTRODUCTION

The present project aims at the acquisition, processing, and interpretation of magnetic data along with the region of the Southern Borborema Province, in the basement adjacent to the Sergipe-Alagoas Sedimentary Basin. The magnetic and geological studies were developed simultaneously and throughout the course of the project in order to make a magnetic modeling of the crustal domains and their tectonic relationships. With them, they seek to construct a model of the geothermal structure of the crust to allow to extrapolate the point data of geothermal flow and to construct a map of geothermal flow for the region.

For the study, we used aeromagnetic data provided by the Geological Survey of Brazil [1]. The development of these databases commonly involves merging numerous surveys with aeromagnetic data with highly variable specifications and quality. For regional exploration, magnetic measurements are important in understanding the tectonic environment. For example, continental boundaries of terrain are commonly recognized by magnetic contrast in all contact [2]. Such regional interpretations require continental scale for magnetic databases.. Thus, it is generally possible to estimate the depth of the sources under favorable circumstances, quantitatively map structures such as faults and blocks, knowing the magnetic anomaly we can estimate the magnetic susceptibility contrast on the subsurface with the depth [3].

The first part of the study consisted in the estimation of the depth of the main domains and Curie point in the study region from the spectral analysis of magnetic anomalies. The knowledge of the Curie depth allows the subsequent estimation of the geothermal gradient and thermal flow in the region. The results obtained from the analysis of the magnetic anomalies were compared to the available geothermal data for this area, demonstrating the potential of the methods for a geothermal evaluation at the regional scale.

Spectral analysis has been applied in the interpretation of gravimetric and magnetic anomalies. The statistical method is used in the interpretation of magnetic anomalies, allowing determining the average depth of all source bodies (magnetic layer) in a given region, according to profile or mapping. In the spectral analysis of magnetic anomalies the depth of the base of the magnetized crust is generally interpreted as the depth of the Curie point, allowing an estimation of the crustal average geothermal gradient [3,4]. In this paper, it was used the Source Parameter Imaging (SPI) method to compute source parameters from gridded magnetic data [5], where the solution grids showed the edge locations and depths.

The study of structure basin is an important economic application of magnetic research, especially in oil and gas exploration. Most of the filling of the basin usually has a much lower susceptibility than the crystalline basement. Thus, it is generally possible to estimate the depth of basement under favorable circumstances, quantitatively map structures such as faults and blocks.

Since such structures in shallow sections often reside on the basement, at least in some depth, and failures in shallow sections are often controlled by the reactivation of basement faults, it is often possible to identify structures favorable to the accumulation of hydrocarbons from the interpretation of the basement. Knowing the magnetic anomaly we can estimate the magnetic susceptibility contrast on the surface of the basin with the depth. In hydrocarbon exploration, such techniques can be used to help correlate complex systems for fault finding or development reservoir [6]. In areas where the layers carry a magnetic signature and plunge at a significant angle, a detailed magnetic investigation can be used to map the very precise surface geology.

## 2. GEOLOGIC CONTEXT

This Southern Borborema Province and the basement adjacent to the Sergipe-Alagoas Sedimentary Basin is located in northeast Brazil, between the Pernambuco Lineament and the NE-N margin of the São Francisco-Congo Craton, being divided into 4 sub-areas: mobile belts Rio Preto, Riacho Pontal, Sergipana and the Pernambuco-Alagoas terrain / massif, interest of the present study [7]. The regional plot of the Pernambuco-Alagoas Terrain (TPEAL) is formed by a Paleoproterozoic gneiss-migmatitic basement [8,9] by a supracrustal and metaplutonic tonian belt, Cabrobó and Belém complexes [10,11], also distinguishing tonian intrusive [12,13]. This set of rocks of amphibolite facies is intruded by several granitic plutons of batolytic dimensions. Some restricted Achaean nuclei are known in the western part of the terrain [14,15].

According to [15], the main units of TPEAL are: i) Orthogneisses and migmatites of granite meta tonalitic composition of varied nature of the Belém Complex of São Francisco and ii) supracrustal rocks rich in biotite and granada, quartzites, amphibolite calcificsilic rocks and locally migmatized orthogneisses of the Cabrobró Complex. [16] identified a series of late-tectonic granites ranging from calcium-alkaline to K-richer members, which may include the shishonite series. These rocks occupy mainly the portion E of the terrain, being called batholiths Buíque-Paulo Afonso, Águas Belas-Canindé and Ipojuca-Atalaia). The predominance of a transpressive deformational tectonic represents the most important structural feature of this terrain, as demonstrated by [17,18].

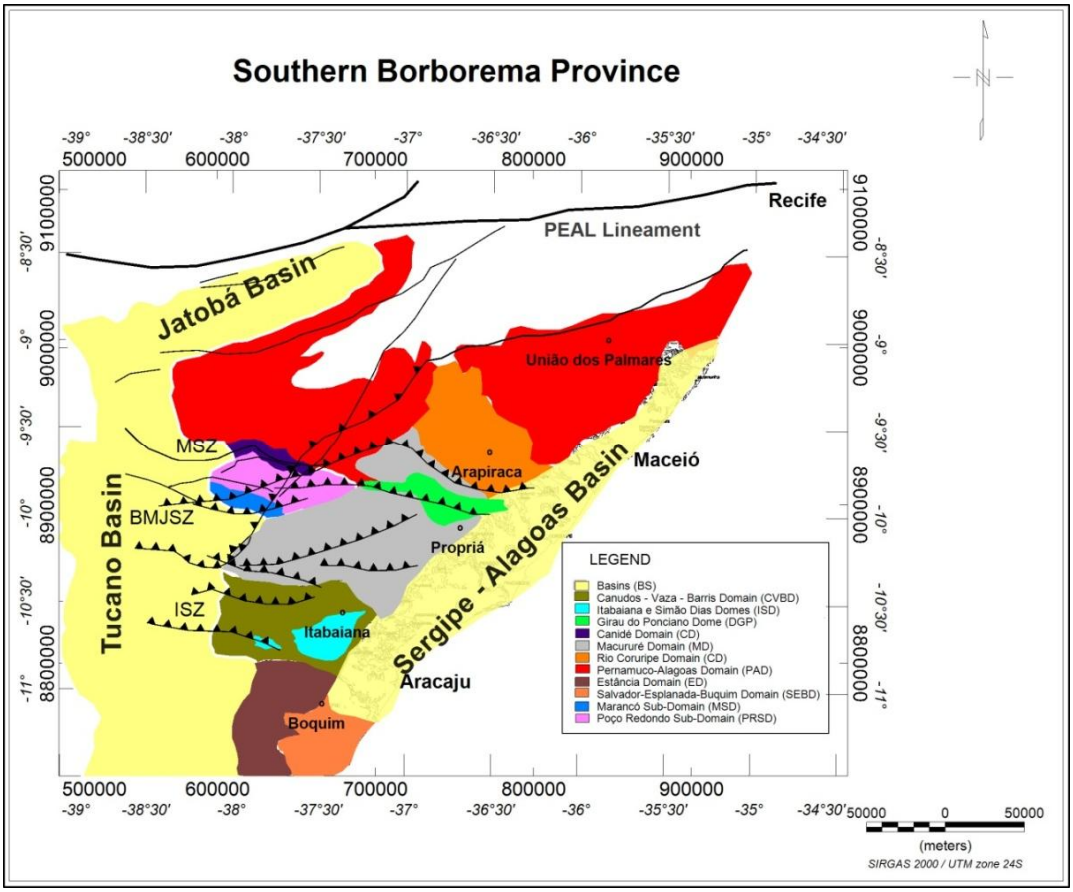


**Fig. 1. Geologic map that shows the region examined in this study and identifies the main regional structures and tectonic domains**

The Sergipana Belt occupies the Southern Domain, being the result of the collision between the Pernambuco-Alagoas terrain to the north and the São Francisco Craton to the south [19]. The tectonic evolution of the Sergipana Belt is characterized by a series of contractionary allochthonous slices, stacked from north to south on the north shore of the San Francisco Craton. In general, it is accepted the subdivision of this band into tectonic domains known as: Canindé, Poço-Redondo-Marancó, Macururé, Vaza Barris and Estância, which are separated by important Neoproterozoic shear zones such as Macururé, Belo Monte-Jeremoabo and Itaporanga [20,21,22].

The Poço Redondo-Marancó and Canindé domains represent, respectively, the registration of a Tonian magmatic arc (979-952 Ma) of the Cariris Velhos orogenic cycle and a subsequent continental extension of Brazil, being composed of plutonic, volcanic and metasedimentary rocks. On the other hand, the Macururé, Vaza-Barris and Estância domains are age Ediacaran, being formed by homonymous supracrustal rocks that present incipient to moderate metamorphism.

The Sergipano Belt is often considered to be the product of a continental collision between the PEAL Domain and the São Francisco Craton [17, 21,19,22]. Given the overall southward vergence of the Sergipano Belt, the São Francisco Craton should represent the lower plate whereas the PEAL Domain would constitute the upper plate. Tthe Macururé Complex and the low-grade to unmetamorphosed domains of the southern Sergipano Belt correspond to distal and proximal facies, respectively, of platform sediments deposited onto the passive continental margin of the São Francisco Craton. In his model, the suture zone separating the two plates would be located close to the transition zone.

[22] questioned this interpretation on the basis that the zircon age population of c. 1000 Ma in the Macururé Domain favors provenance from the Borborema Province. Furthermore, 600-570 Ma-old zircons in the upper units of the southern sequences of the Sergipana Belt would indicate derivation from sources formed during the Brasilian Orogeny, such that they are best interpreted as foreland sediments. In order to explain the younger zircon population (680-660 Ma) and the intraplate affinities of associated magmatic rocks in the Canindé Complex, they proposed extension of the PEAL Domain before collision, and placed the suture between this domain and the São Francisco Craton much more to the south than the location proposed by [21]. In their model, between 630 and 615 Ma, seduction of the oceanic lithosphere of the São Francisco plate led to arc magmatism, inversion of the Canindé rift, and closing of the ocean separating the two continental plates.

Both of the above models assume the existence of a large ocean between the São Francisco Craton and the Borborema Province before the Brasiliano Orogeny. However, none of the features expected from a collisional event following oceanic closure are supported by the data obtained in this study and in previous works.

## 3. MATERIALS AND METHODS

The aeromagnetic projects have a spacing of flight lines of 500 m oriented in the N-S direction, with flight height of 100 m on the ground, the interval between measurements of the magnetometer of 0.1 s and the spectrometer 1.0 s. The magnetic data of the study area generated from the pre-processed data, using different combinations of lighting parameters, the cell size of 1/4 of the flight line [23,24]. Grids of the magnetic anomaly were generated (Fig. 2) and then a database of each grid generated and a rectangle was cut around the Sergipe-Alagoas Basin defining the study area.

Usual linear transformations were applied to the magnetic data to process changes in the amplitude and/or phase related to the set of sine waves that constitute the entire grid of the data. These transformations are carried out by multiplying the Fourier transform in the data set in the frequency domain. The inverse Fourier transform returns to the space domain and gives the current field to the upper level. This is equivalent to convolving the field in the space domain by an operator (or filter). All transformations of the magnetic field work on this path.

The calculation of the field at higher levels is called continuation upwards and proposes the removal of high-frequency anomalies relative to low-frequency anomalies. The process can be used to suppress the effect of shallower anomalies when detailing deeper anomalies is desired. The effect of the amplitude of the analytical signal is to highlight the edges of the sources of the anomalies and is very useful in the case of magnetic data that contain the influence of magnetization remaining or taken at

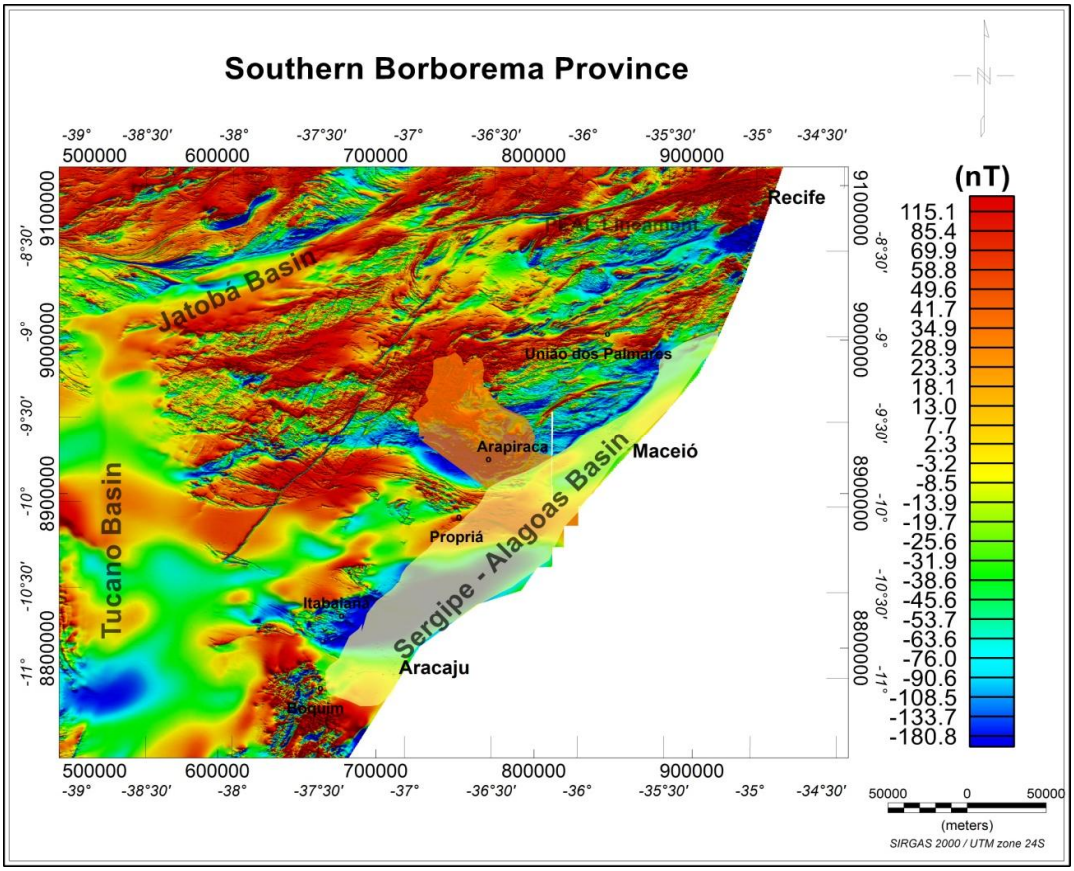


**Fig. 2. The aeromagnetic data represented in the integrated magnetic anomaly map (nT)**

low magnetic latitudes. The amplitude of the analytic signal is the symmetric sine-shaped function with exactly the top of each contact and width directly related to the depth of the body.

## 4. IMAGE EDGE DETECTION

Magnetic maps are frequently used to delineate geologic contacts and border of geological formation. These maps have signals with various amplitudes that originate from different geometric sources, situated at different depths and with different magnetic properties. The vertical derivative has been used for many years to delineate edges in magnetic field data [25,26,5].

Many filters commonly used to enhance subtle detail in the magnetic field are based on combinations of the horizontal and vertical derivatives of the data set. In recent years, improved methods have been developed rapidly. For instance, the tilt angle (TDR) [27], the Theta map [28], the total horizontal derivative of the tilt angle as an edge detector (THDR) [29], the horizontal tilt angle (TDX) [30], the balanced analytic signal [31] and the normalized horizontal derivative [32]. The study of [30] applied the various local phase-based filters on aeromagnetic data from Australia. [31] introduced the terracing method as an operator that is applied to potential field data to produce regions of constant field amplitude that are separated by sharp boundaries. [33] showed the efficiency of the tilt angle of the horizontal gradient for qualitative interpretation of magnetic data. A derivative operator was introduced by [34] based on the tilt angle of the horizontal and vertical derivatives of the total horizontal gradient of gravity data set, normalized by the analytic signal amplitude (THA).

A commonly used edge-detection filter is the total horizontal derivative (THDR) which is given by [30]

$$THDR = \sqrt{\left(\frac{\partial T}{\partial x}\right)^2 + \left(\frac{\partial T}{\partial y}\right)^2} \quad (1)$$

T is the magnetic anomaly. The total horizontal derivative (THDR) of the study area is showed in Fig. 3.

The amplitude of the analytic signal or total gradient is a commonly used filter that produces bell-shaped anomalies over magnetic bodies [35].

The analytic signal is a linear combination of horizontal and vertical derivatives whose amplitude is given by:

$$AS = \sqrt{\left(\frac{\partial T}{\partial x}\right)^2 + \left(\frac{\partial T}{\partial y}\right)^2 + \left(\frac{\partial T}{\partial z}\right)^2} \quad (2)$$

This filter enhances edges of features of all azimuths. [27] introduce the tilt angle that is ratio of the vertical derivative to the a value of the total horizontal derivative which is defined as

$$TA = \arctan\left(\frac{\partial T / \partial z}{THDR}\right) \quad (3)$$

If the density contrast is positive, the tilt angle value is positive when over the source, passes through zero when over, or near, the edge where the vertical derivative is zero and the horizontal derivative is a maximum and is negative outside the source region [30,23,24].

The tilt angle has a range of -90˚ to +90˚ and is much simpler to interpret than the analytic signal phase angle [30].

The authors [36] presented an edge detection method that is based on the enhancement of the THDR of magnetic anomalies using the TA. It is referred to as the tilt angle of the horizontal gradient (TAHG) method:

$$TAHG = \arctan\left[\frac{\partial THDR / \partial z}{\sqrt{\left(\frac{\partial THDR}{\partial x}\right)^2 + \left(\frac{\partial THDR}{\partial y}\right)^2}}\right] \quad (4)$$

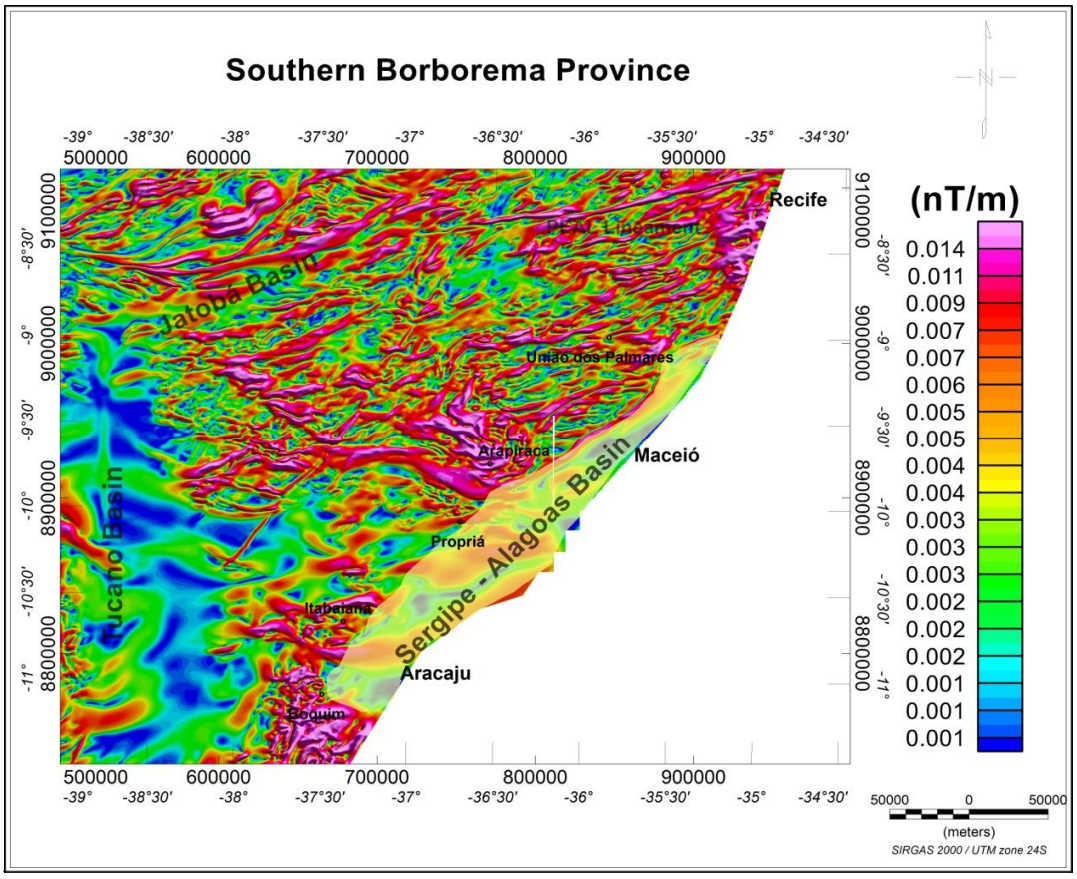


**Fig. 3. The aeromagnetic data represented in terms of gradient horizontal total (nT/m), main magnetic lineaments, shear, and subduction zones**

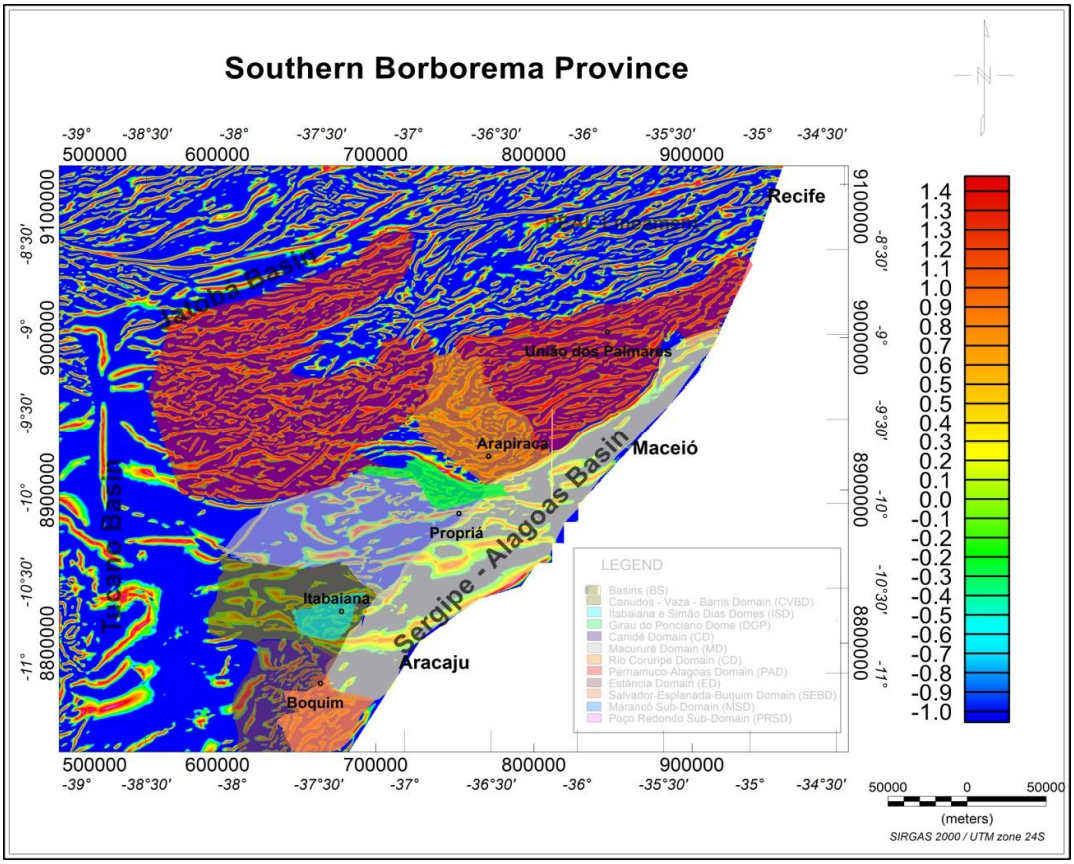


**Fig. 4. The aeromagnetic data represented in terms of the analytical signal of the gradient horizontal total, main magnetic lineaments, shear, and subduction zones**

In this study, efficiency of the TAHG is considered for gravity data set. The TAHG transform range is from $-\pi/2$ to $+\pi/2$.

## 5. DEPTH SOLUTIONS

The Source Parameter Imaging (SPI) method computes source parameters from gridded magnetic data [5]. The method assumes either a sloping contact or a dipping thin-sheet model and is based on the complex analytic signal. Solution grids show the edge locations and depths. The estimate of the depth is independent of the magnetic inclination, declination, dip, strike and any remanent magnetization; however, the dip and the susceptibility estimates do assume that there is no remanent magnetization.

Image processing of the source-parameter grids enhances detail and provides maps that facilitate interpretation.

SPI assumes a step-type source model. For a step, the following formula holds:

$$Depth = \frac{1}{Kmax} \tag{5}$$

where Kmax is the peak value of the local wavenumber K over the step source.

$$K = \sqrt{\left(\frac{\partial TA}{\partial x}\right)^2 + \left(\frac{\partial TA}{\partial y}\right)^2} \tag{6}$$

where TA is Tilt derivative (eq. 3). SPI method first computes TA and K. Then it finds peak values $K_{max}$ using the Blakely test. These peak values are used to compute depth solutions, which saved to a database.

The SPI to compute the two horizontal derivative grids in the space-domain, and the first vertical derivative grid in the frequency-domain, using the standard filters. However, the user may compute these grids separately if desired.

We applied a smoothing (Hanning) filter to the K grid to reduce noise before calculating the source

depths. The default is zero (no Hanning filter). More passes tend to reduce the number of shallow solutions found.

We use the [37] method to find localized peaks in a grid. For each grid cell to be considered, the SPI code compares its value with the eight surrounding grid cells in four directions (x-direction, y-direction, and both diagonals). There are four levels to determine whether a grid cell can be selected as a peak. Any solutions deeper than this cutoff level were rejected.

## 6. RESULTS OF CURIE DEPTH FROM MAGNETIC DATA

The Curie point (or Curie temperature) consists of the temperature at which a ferromagnetic material loses its magnetizing capacity and starts to have a paramagnetic behavior. Magnetic minerals come from the iron-titanium-oxygen geochemical groups, the series of titanomagnetites (magnetite and ulvospinela) and the series titanohematites (ilmenite and hematite), and ferro-sulfur (pyrrotite and greigite).

The magnetic properties of igneous and metamorphic rocks depend on their composition, oxidation state, hydrothermal alteration and metamorphic conditions [38]. The magnetic behavior of the rocks is usually dependent on the magnetite content, since this is the most common magnetic mineral, with a Curie temperature generally being given between 500 and 600°C (580°C for pure magnetite). The increase in titanium (Ti) content in the rocks promotes Curie temperature decrease, and it is more realistic to admit one of 500 to 550°C for magnetite [3]. A temperature of 560°C may be allowed at the depth of the granite body base [39].

Spectral analysis has been applied in the interpretation of gravimetric and magnetic anomalies. The statistical method of [40] is used in the interpretation of magnetic anomalies, allowing determining the average depth of all source bodies (magnetic layer) in a given region, according to profile or mapping [3,41,42]. In the spectral analysis of magnetic anomalies the depth of the base of the magnetized crust is generally interpreted as the depth of the Curie point, allowing an estimation of the crustal average geothermal gradient [43,42]. In this paper, we used SPI method to compute the source edge locations and depths from gridded magnetic data [5].

The study of basin structure was important to magnetic research, especially in oil and gas exploration. The sedimentary basin usually has a much lower susceptibility than the crystalline basement.

Thus, it is generally possible to estimate the depth of basement under favorable circumstances, quantitatively map structures such as faults and blocks. From the slope of the power spectrum, the upper bound ($Z_T$) and the centroid ($Z_0$) depth of a magnetic body can be estimated. The lower bound of the magnetic source can be derived [42,4] as:

$$Z_b = 2 \cdot Z_0 - Z_T \tag{7}$$

Since $Z_b$ is the lower bound depth of the magnetic body, it suggests that ferromagnetic minerals are converted to paramagnetic minerals due to temperature of approximately 580°C. Therefore, the obtained bottom depth of the magnetic source, $Z_b$, was assumed to be the Curie point depth.

In order to relate the Curie point depth ($Z_b$) to Curie point temperature (580°C), the vertical direction of temperature variation and the constant thermal gradient were assumed. The geothermal gradient (dT/dz) between the Earth's surface and the Curie point depth ($Z_b$) can be defined by Eq. (7) [4]:

$$\frac{dT}{dz} = \frac{580\,^{\circ}C}{Z_b} \tag{8}$$

Further, the geothermal gradient can be related to the heat flow *q* by using the formula [4]:

$$q = \gamma \frac{dT}{dz} = \gamma \frac{580^{\circ}}{Zb} \tag{9}$$

where $\gamma$ is the coefficient of thermal conductivity. From Eq. (9), the Curie point depth is inversely proportional to heat flow.

The Curie point depth ($Z_b$) was estimated by spectral analysis and SPI method of magnetic anomaly data of Southern Borborema Province. The present result was compared with the tectonic and heat flow data. The $Z_b$ Fig. 5 shows the Curie point depth of from the 13 up to 33 km. The Curie point depth indicates the bottom depth

of magnetic sources and reflects the thermal gradient and the observed heat flow data. The Fig. 6 shows that the thermal gradient varies from the 15°C/km up to 35°C/km. The Fig. 7 shows that the heat flow varies from the 38 mW/m² up to 90 mW/m² heat flow.

Comparing the Curie point depth map with the heat flow in Fig. 8 we can see that the values have a good correlation as expected by Eq. 9. Knowing the magnetic anomaly it was possible to estimate the depth top and bottom of the main geologic domain in the study area (Table 1).

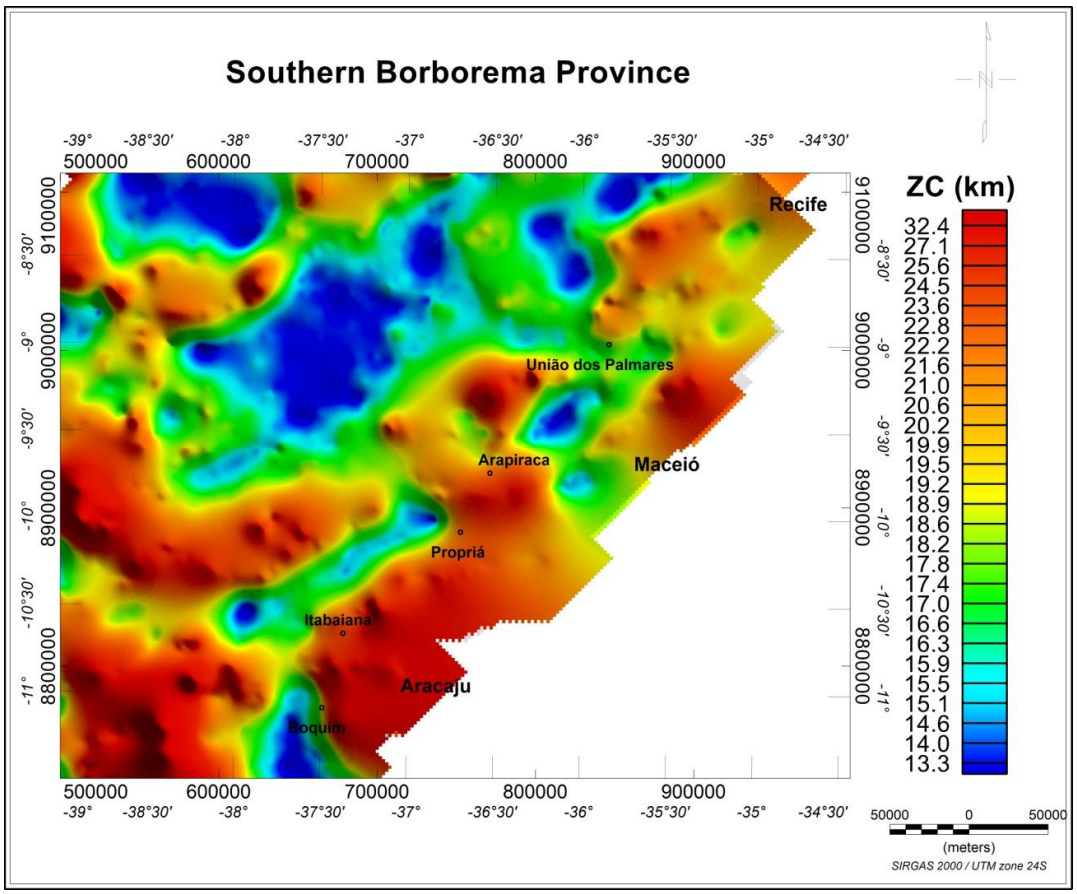


**Fig. 5. Curie point depth ($Z_b$) map and sedimentary basins boundary**

**Table 1. Tectonic domains of the Southern Borborema Province e results of the top depth ($Z_T$), bottom depth ($Z_0$), Curie point depth ($Z_b$) and heat flow data (Q) from magnetic data**

| Geologic domain | X (m) | Y (m) | $Z_T$ (km) | $Z_0$ (km) | $Z_b$ (km) | Q (mW/m²) |
|---|---|---|---|---|---|---|
| Rio coruripe | 745049 | 8944354 | 3,3 | 15,0 | 26,7 | 54,3 |
| Rio coruripe | 744767 | 8944482 | 3,3 | 15,0 | 26,7 | 54,3 |
| Rio coruripe | 749873 | 8929955 | 3,4 | 16,0 | 28,6 | 50,7 |
| Peal | 259052 | 9165398 | 2,9 | 15,0 | 27,1 | 53,5 |
| Peal | 260957 | 9167322 | 2,9 | 14,2 | 25,5 | 56,9 |
| Peal | 201175 | 8973671 | 4,2 | 14,1 | 24,0 | 60,4 |
| Domo itabaiana | 669848 | 8820926 | 3,0 | 16,9 | 31,0 | 46,8 |
| Vaza-barris | 623505 | 8822970 | 3,3 | 11,5 | 19,7 | 73,6 |
| Estância | 614776 | 8759932 | 3,7 | 14,1 | 24,5 | 59,2 |
| Macururé | 711300 | 8892007 | 3,5 | 13,0 | 22,5 | 64,4 |
| Salvador-esplanada-boquim | 647680 | 8763205 | 2,9 | 13,1 | 23,3 | 62,2 |

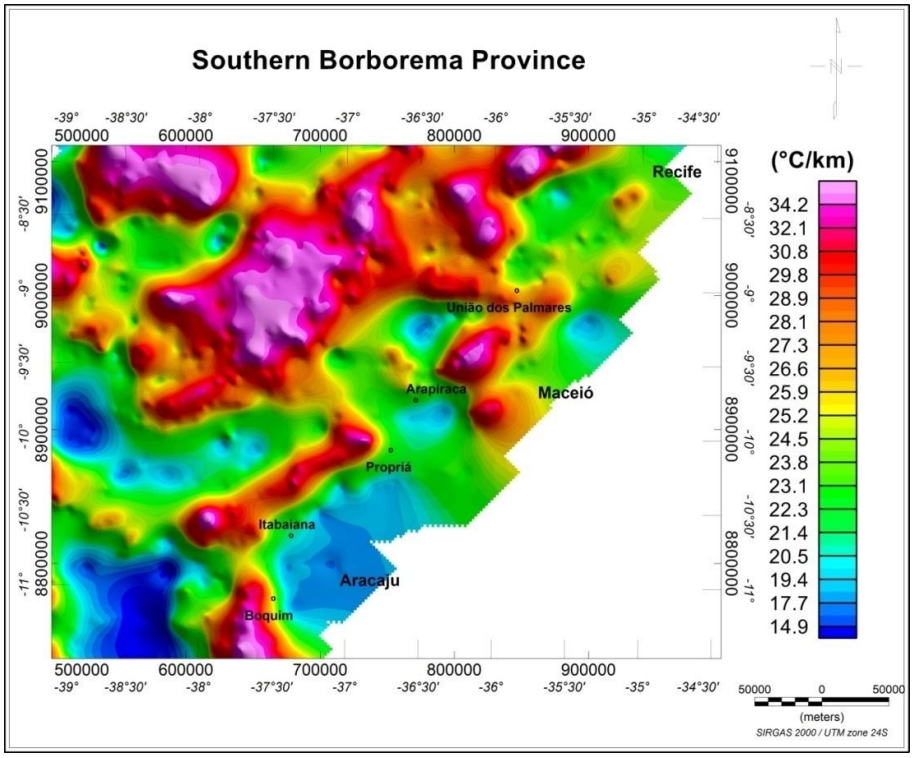


**Fig. 6. Thermal gradient map derived from Curie point depth map (Curie temperature 580C)**

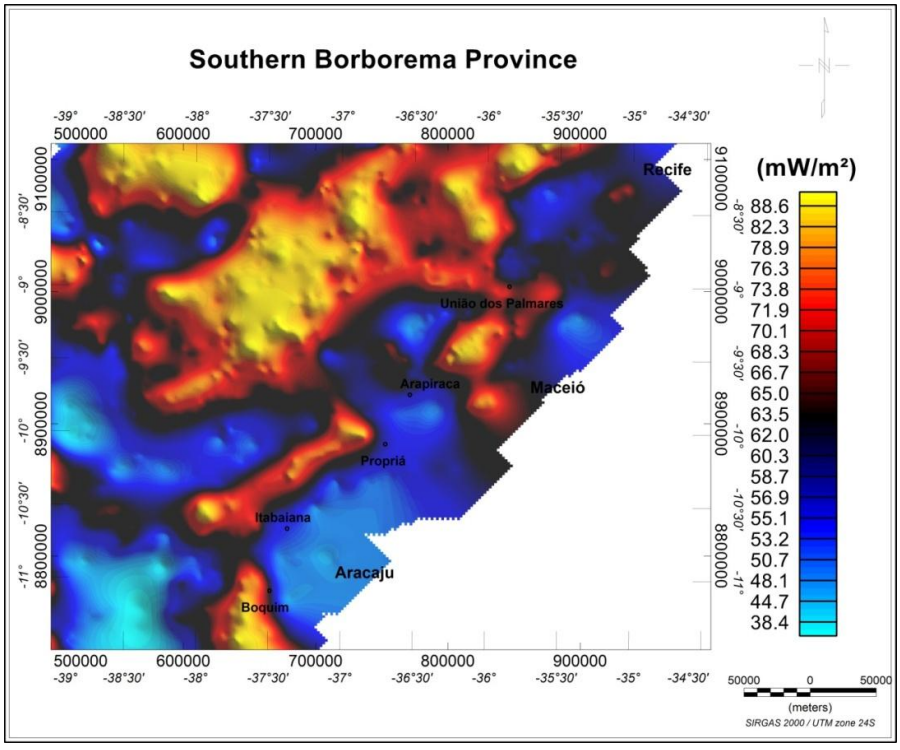


**Fig. 7. Heat flow map derived from Curie point depth (thermal conductivity 2.978 $Wm^{-1}K^{-1}$)**

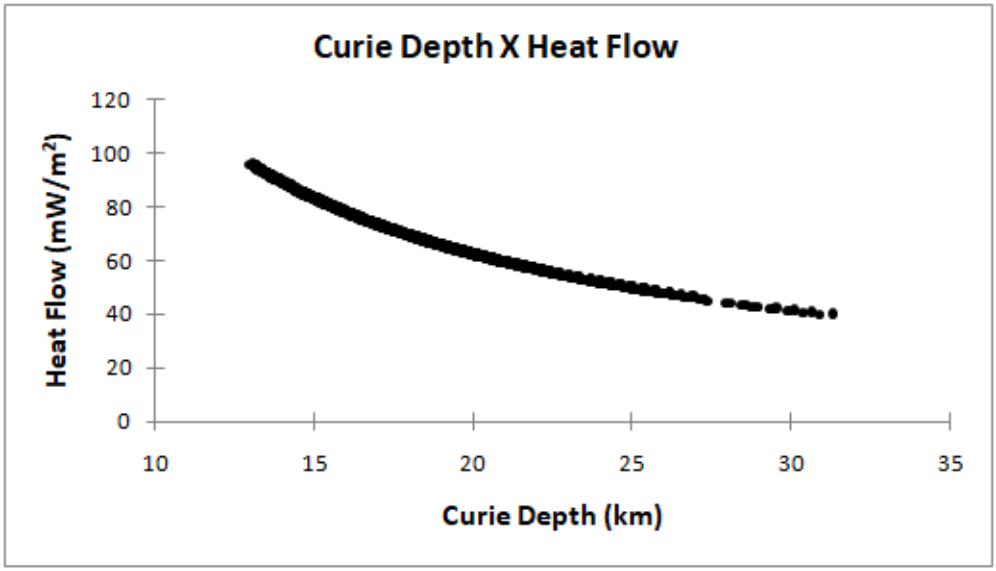


**Fig. 8. Relationship between Curie point depth and heat flow data from magnetic data**

## 7. DISCUSSION

We can produce a geological interpreting and understanding the tectonic environment. The magnetic measurements were important for continental boundaries of terrain were commonly recognized by magnetic contrast in all contact. The structures in shallow sections often reside on the basement, at least in some depth, and failures in shallow sections are often controlled by the reactivation of basement faults, it is often possible to identify structures favorable to the accumulation of hydrocarbons from the interpretation of the basement. The techniques could be used to help correlate complex systems for fault finding or development reservoir.

The results show a change in depth of the sources in which in the northern part of the study area are deeper and the southern sources in the region are shallower. As the region of is a collision area of blocks. The PEAL domain has a different composition from the rest of the region. The main units of PEAL were orthogneisses and migmatites of granite metatonalitic composition and supracrustal rocks rich in biotite and granada, quartzites, amphibolite calcificsilic rocks and locally migmatized orthognaisses. As can be seen by the important magnetic lineaments mapped in Fig. 4, where the main lineaments and lateral contacts between the blocks were marked along the magnetic relief. Ancient subduction zones were marked enterirmentes presented in [44].

The Sergipana Belt occupies the Southern Domain, being the result of the collision between the PEAL terrain to the north and the São Francisco Craton to the south. A series of contractionary slices, stacked from north to south on the north shore of the San Francisco Craton are also well marked along the region's magnetic relief. We can identify different lineaments and magnetic structures that demarcate the tectonic limits of the subdivision of this band into domains known as Macururé, Vaza Barris and Estância, which are separated by important neoproterozoic shear zones such as Macururé, Belo Monte-Jeremoabo and Itaporanga (Figs. 3 e 4). The Macururé, Vaza-Barris and Estância domains are formed by supracrustal rocks that present moderate metamorphism.

## 8. CONCLUSION

The development of the databases involved merging numerous surveys with aeromagnetic data with highly variable specifications and quality. The integrated and corrected magnetic anomaly maps (Fig. 2) were processed and interpreted. Knowing the magnetic anomaly it was possible to estimate the depth top and bottom, magnetic lineaments, faults, blocks, the lateral extension, the width of the sources. From these results, we can produce a geological interpreting and understanding the tectonic environment. For regional exploration, magnetic measurements were important for example, continental boundaries of terrain were commonly

recognized by magnetic contrast in all contact. Such regional interpretations required continental scale for magnetic databases.

The Curie depth varies from the 13 up to 33 km and the heat flow varies from the 38 mW/m² up to 90 mW/m² heat flow. The crustal depth region is characterized by roughly constant gradients through the upper crust (0–16 km) and lower-but-changing gradients in the lower crust. The upper-crust gradients for a given heat flow remain almost constant because the effect of reduced heat flow due to radioactivity in the crust is counteracted by a decrease in thermal conductivity with an increase in temperature.

The hottest thermal states, characterized by the geotherms for surface heat flow values of 80 and 90 mW/m², could provide for deep crustal melting under hydrous conditions; dry melting in the crust of typical thickness appears to be precluded in regions where these steady-state, static geotherms apply. [45] argued that a lack of complete overlap between the geotherms and the metamorphic P-T space requires dynamic tectonic processes, such as subduction (low T, high P) or magmatic processes (high T, low P), that can be considered perturbations to the framework geotherms.

The thermal event and the effects are seen at the surface; in many tectonic scenarios, however, the thermal effect is initially near-surface (e.g., erosion, burial, thrusting), so the importance of any time shifts may be different. There are fundamental physical differences between oceans and continents in terms of the underlying sources of the lithospheric addition to basal heat flow. Understanding these differences is an important component of seeing through of lithospheric heat production to image heat transfer and temperature structure in the upper mantle.

## COMPETING INTERESTS

Authors have declared that no competing interests exist.

## REFERENCES


1. CPRM. Projeto Aerogeofísico Borda Leste do Planalto da Borborema, CPRM (Programa Geologia do Brasil); 2008.
2. Casas-Sainz AM, Román-Berdiel T, Oliva-Urcia B. Multidisciplinary approach to constrain kinematics of fault zones at shallow depths: A case study from the Cameros–Demanda thrust (North Spain). Int J Earth Sci (Geol Rundsch). 2017;106:1023–1055. Available:https://doi.org/10.1007/s00531-016-1349-5
3. Hinze WJ, von Frese RRB, Saad AH. Gravity and magnetic exploration: Principles, practices, and applications. Cambridge University Press, Editor: Dr. Susan Francis, ISBN: 9780521871013; 2013.
4. Tanaka A, Okubo Y, Matsubayashi O. Curie point depth based on spectrum analysis of the magnetic anomaly data in East and Southeast Asia. Tectonophysics. 1999;306:461-470.
5. Thurston JB, Smith RS. Automatic conversion of magnetic data to depth, dip and susceptibility contrast using the SPITM method. Geophysics. 1997;62:807-813.
6. Brink HJ. The evolution of the North German Basin and the metamorphism of the lower crust. Int J Earth Sci (Geol Rundsch). 2005;94:1103–1116. Available:https://doi.org/10.1007/s00531-005-0037-7
7. Brito Neves BB, Santos EJ, Schmus WRV. Tectonic history of the Borborema Province. In: Umberto Cordani; Edson Jose Milani; Antonio Thomaz Filho; Diogenes de Almeida Campos. (Org.). Tectonic Evolution of South America. Rio de Janeiro: 31st International Geological Congress. 2000;151-182.
8. Accioly ACA. Geologia, Geoquímica e significado Tectônico do Complexo Metanortosítico de Passira-Província Borborema-Nordeste Brasileiro. 168 p. Tese Doutorado - Programa de Pós-graduação em Geoquímica e Geotectônica, USP, São Paulo; 2000.
9. Neves SP. Tectonic evolution of the Borborema province: Constrains from zircon geochronology. J. S. Am. Earth Sci. 2015;58:150-164.
10. Brito Neves BB, Van Schmus WR, Santos EJ, Campos Neto MC, Kozuch M. O Evento Cariris Velhos na Província Borborema: Integração de dados, implicaçoes e perspectivas. Rev. Bras. Geociências. 1995;25:279-296.
11. Santos EJ. Ensaio preliminar sobre terrenos e tectônica acrecionária na Província Borborema. In: SBG, Congresso Brasileiro de Geologia, 390, Salvador, Proceedings. 1996;47-50.

12. Cruz RF, Accioly ACA. Petrografia, geoquímica e idade U-Pb do Ortognaisse Rocinha, no domínio Pernambuco-Alagoas - W da Província Borborema. Estud. Geol. 2013;23:3-27.
13. Lima MMC. Caracterização geoquímica, isotópica e geotectônica dos Complexos Araticum e Arapiraca, Faixa Sergipana, Alagoas, Nordeste do Brasil. Dissertação de mestrado. UFPE, Recife; 2013.
14. Cruz RF, Pimentel MM, Accioly ACA. Provenance of metasedimentary rocks of the western Pernambuco-Alagoas domain: Contribution to understand the Neoproterozoic tectonic evolution of southern Borborema Province. J. S. Am. Earth Sci. 2015;58:82-99.
15. Delgado IM, Souza JD, Silva LC, Silveira Filho NC, Santos RG, Pedreira AJ, Guimarães JT, Angelim LAA, Vasconcelos AM, Gomes IP, Lacerda Filho JV, Valente CR, Perrotta MM, Heineck CA. Geotectônica do Escudo Atlântico. In: Bizzi LA, Schobbenhaus C, Vidotti RM & Gonçalves JH (Eds.). Geologia, tectônica e recursos minerais do Brasil: texto, mapas & SIG. CPRM. 2003;227-334.
16. Silva Filho AF, Guimaraes IP, Brito MFL, Pimentel MM. Geochemical signatures of main neoproterozoic late-tectonic granitoids from the Sergipano Fold belt, Brazil: Significance for the Brasiliano Orogeny. International Geology Review, Estados Unidos. 1997;39(7):639-659.
17. Brito Neves BB. Regionalização Geotectônica Do Pre-cambriano Nordestino (Tese). Universidade de São Paulo, São Paulo; 1975.
18. Santos EJ. O complexo granítico Lagoa das Pedras: Acresção e colisão na região de Floresta (Pernambuco), Província Borborema (PhD Thesis). Instituto de Geociências da Universidade de São Paulo. 1995;228.
19. Oliveira EP, Toteu SF, Araújo MNC, Carvalho MJ, Nascimento RS, Bueno JF, McNaughton N, Basilici G. Geologic correlation between the neoproterozoic Sergipano belt (NE Brazil) and the Yaound e belt (Cameroon, Africa). J. Afr. Earth Sci. 2006;44:470-478.
20. Davison I, Santos RA. Tectonic evolution of the Sergipano Fold Belt, NE Brazil, during the brasiliano orogeny. Precambrian Research. 1989;45:319-342.
21. D'el Rey Silva LJH. The evolution of basement gneiss domes of the Sergipano fold belt (NE Brazil) and its importance for the analysis of Proterozoic basins. Journal of South American Earth Sciences. 1995;8(3/4):325-340.
22. Oliveira EP, Windley BF, Araújo DB. The Neoproterozoic Sergipano orogenic belt, NE Brazil: A complete plate tectonic cycle in western Gondwana. Precambrian Res. 2010;181:64-84.
23. Cooper GRJ, Cowan DR. Edge enhancement of potential-field data using normalized statistics. Geophysics. 2008;73(3):H1–H4.
24. Cooper GRJ, Cowan DR. Terracing potential field data. Geophysical Prospecting. 2009;57:1067–1071.
25. Evjen HM. The place of the vertical gradient in gravitational interpretations. Geophysics. 1936;1:127–136.
26. Hood PJ, Teskey DJ. Aeromagnetic gradiometer program of the Geological Survey of Canada. Geophysics. 1989;54(8):1012–1022.
27. Miller HG, Singh V. Potential field tilt - a new concept for location of potential field sources. Journal of Applied Geophysics. 1994;32:213–217.
28. Wijns C, Perez C, Kowalczyk P. Theta map: Edge detection in magnetic data. Geophysics. 2005;70:39–43.
29. Verduzco B, Fairhead JD, Green CM. New insights into magnetic derivatives for structural mapping. The Leading Edge. 2004;23(2):116–119.
30. Cooper GRJ, Cowan DR. Enhancing potential field data using filters based on the local phase. Computers and Geosciences. 2006;32:1585–1591.
31. Cooper GRJ. Balancing images of potential field data. Geophysics. 2009;74: L17–L20.
32. Ma G, Li L. Edge detection in potential fields with the normalized total horizontal derivative. Computers and Geosciences. 2012;41:83–87.
33. Ferreira FJF, Castro LG, Bongiolo ABS, Castro LG. Enhancement of the total horizontal gradient of magnetic anomalies using the tilt angle. Geophysics. 2013;78: J33–J41.
34. Eshaghzadeh A. Anomaly edge enhancement of microgravity data using normalized standard deviation. Geodynamics Research International Bulletin, 2, XLVIIILII; 2014.

35. Nabighian MN. The analytical signal of 2D magnetic bodies with polygonal cross-section: Its properties and use for automated anomaly interpretation. Geophysics. 1972;37:507–517.
36. Ferreira FJF, Castro LG, Bongiolo ABS, Souza J, Romeiro MAT. Enhancement of the total horizontal gradient of magnetic anomalies using tilt derivatives: Part II—Application to real data. 81st Annual International Meeting, SEG, Expanded Abstracts. 2011;887–891.
37. Blakely RJ, Simpson RW. Approximating edges of bodies from magnetic or gravity anomalies. Geophysics. 1986;51:1494-1498.
38. Just J, Kontny A. Thermally induced alterations of minerals during measure-ments of the temperature dependence of magnetic susceptibility: A case study from the hydrothermally altered Soultz-sous-Forêts granite, France. Int J Earth Sci (Geol Rundsch). 2012;101:819–839. Available:https://doi.org/10.1007/s00531-011-0668-9
39. Shuey RT, Schellinger DK, Tripp AC, Alley LB. Curie depth determination from aeromagnetic spectra. Geophysical Journal of the Royal Astronomical Society. 1977;50:75-101.
40. Spector A, Grant FS. Statistical models for interpreting aeromagnetic data. Geophysics. 1970;35:293-302.
41. Negi JG, Agrawal PK, Pandey OP. Large variation of Curie depth and lithospheric thickness beneath the Indian subcontinent and a case for magnetothermometry. J. Geophys. 1. R. Astr. Soc. 1987;88:763-775.
42. Okubo Y, Graf RJ, Hansen RO, Ogawa K, Tsu H. Curie point depth of the island of Kyushu and surrounding areas, Japan. Geophysics. 1985;53:481-494.
43. Bhattacharyya BK, Leu LK. Analysis of magnetic anomalies over Yellowstone National Park: Mapping of Curie point isothermal surface for geothermal reconnaissance. Journal of Geophysical Research. 1975;80:4461-4465.
44. Neves SP, Bruguier O, Silva JMR, Mariano G. From extension to shortening: Dating the onset of the Brasiliano Orogeny in eastern Borborema Province (NE Brazil). J. S. Am. Earth Sci. 2015;58:238-256.
45. Furlong KP, Chapman DS. Heat flow, heat generation, and the thermal state of the lithosphere. Annu. Rev. Earth Planet. Sci. 2013;41:385–410. DOI:10.1146/annurev.earth.031208.100051



*Peer-review history:*
*The peer review history for this paper can be accessed here:*
*http://www.sciencedomain.org/review-history/23823*